PROTEIN STRUCTURE REPORT

High-resolution crystal structure of human Mapkap kinase 3 in complex with a high affinity ligand

Robert Cheng,[1] Brunella Felicetti,[1] Shilpa Palan,[1] Ian Toogood-Johnson,[1] Christoph Scheich,[2] John Barker,[1] Mark Whittaker,[1] and Thomas Hesterkamp[2]*

[1]Evotec (UK) Ltd, 114 Milton Park, Abingdon, Oxfordshire OX14 4SA, United Kingdom
[2]Evotec AG, Schnackenburgallee 114, 22525 Hamburg, Germany

Received 29 September 2009; Revised 6 November 2009; Accepted 6 November 2009
DOI: 10.1002/pro.294
Published online 20 November 2009 proteinscience.org

Abstract: The Mapkap kinases 2 and 3 (MK2 and MK3) have been implicated in intracellular signaling pathways leading to the production of the pro-inflammatory cytokine tumor necrosis factor alpha. MK2 has been pursued by the biopharmaceutical industry for many years for the development of a small molecule anti-inflammatory treatment and drug-like inhibitors have been described. The development of some of these compounds, however, has been slowed by the absence of a high-resolution crystal structure of MK2. Herein we present a high-resolution (1.9 Å) crystal structure of the highly homologous MK3 in complex with a pharmaceutical lead compound. While all of the canonical features of Ser/Thr kinases in general and MK2 in particular are recapitulated in MK3, the detailed analysis of the binding interaction of the drug-like ligand within the adenine binding pocket allows relevant conclusions to be drawn for the further design of potent and selective drug candidates.

Keywords: tumor necrosis factor alpha (TNFα); lipopolysaccharide; pyrrolo pyridine; construct design; structure-based drug design

Introduction

The p38α Mapkap kinase pathway has been in the center of the quest for novel, nonbiological anti-inflammatory therapeutics, given its dominant role in the generation of a pro-inflammatory, tumor necrosis factor alpha (TNFα) mediated immune response against a variety of environmental challenges.[1] Cellular effector molecules regulated by p38α, among a variety of others, are the Mapkap kinases MK2 and MK3. These are ubiquitous, constitutive components of the pro-inflammatory signal transduction pathway that are considered to be "downstream" enough to avoid the pleiotropic pharmacological effects of p38α inhibitors.[2] MK2 and MK3 share the same list of cellular phosphorylation targets; tristetraproline, CREB, HSF-1, Hsp27 and few others.[3] Knock-out studies in mice have shown a strict requirement for MK2 in the TNFα response to lipopolysaccharide (LPS) challenge. MK2 deficient

Abbreviations: LPS, lipopolysaccharide; MK2/MK3, mapkap kinase 2/3; NES, nuclear export signal; NLS, nuclear localization signal; TNFα, tumor necrosis factor alpha.

Additional Supporting Information may be found in the online version of this article.

Robert Cheng and Brunella Felicetti contributed equally to this work.

**Correspondence to:* Thomas Hesterkamp, Evotec AG, Schnackenburgallee 114, 22525 Hamburg, Germany.
E-mail: thomas.hesterkamp@evotec.com

mice are refractory to the development of collagen-induced arthritis[4] and show a lower incidence of LPS induced endotoxic shock.[5] The MK3 knock-out mouse is without phenotype but the MK2 and MK3 double knock-out shows a relatively stronger TNFα phenotype than MK2$^{-/-}$ alone while being without general growth and fertility defects.[6] Based on this MK2 can be considered the dominant anti-inflammatory target and MK3 the accessory target that may provide some compensatory role in situations of absence (or inhibition) of MK2.

MK2 has been extensively studied by structural biology techniques. This has resulted in a number of relevant structures of wild-type, truncated and point-mutated *apo* MK2, MK2 in complex with ADP and small molecule ligands,[7–11] but also MK2 in a tight complex with p38α.[12] All these structures show maximum resolution levels in the 2.6 to 3.2 Å range and are thus of limited use to reveal precise details of the binding interactions of ligands including pharmaceutical lead compounds. We therefore set out to resolve the structure of MK3 which was hitherto not available within the public domain. The high sequence homology between MK2 and MK3 particularly in the catalytic domain (78% identity), suggests that the MK3 structure could serve as a valuable model for the Mapkap kinase family and the design of MK3 and MK2 inhibitors.

To that end we present the high-resolution crystal structure of human MK3 in complex with a pharmaceutical ligand. Our initial efforts of making crystal-grade MK3 protein based on low throughput protein production methods did not prove to be successful in yielding a suitable construct for structure determination. However, the parallel generation of multiple variants of MK3 has proven rewarding in identifying the one most suitable protein construct yielding highly diffracting crystals.

Results

MK3 construct design and expression studies

Human MK3 consists of 382 amino acids, coding for a proline-rich N-terminal domain, followed by the catalytic kinase domain. The regulatory C-terminus contains an auto-inhibitory region, a nuclear localization signal (NLS) and a nuclear export signal (NES). To generate stable, homogeneous and soluble protein for crystallographic studies we altered systematically the N- and C- termini of the catalytic domain of MK3. This was done with the intent of removing flexible or disordered segments that might hinder crystallization and to provide variants that might enable high resolution crystal forms. We designed constructs spanning either just the catalytic domain or incorporating the regulatory NES and NLS domains in addition to the kinase domain.

Four MK3 constructs (comprising, respectively, amino acids 33–343, 33–345, 33–349, and 35–345) yielded the highest amount of soluble and monodisperse protein. These were purified to homogeneity on larger scale. All four constructs were progressed into sparse matrix crystallization trials and one construct (amino acids 33–349) yielded highly diffracting crystals when in complex with a high-affinity pyrrolopyridinone-based pharmaceutical lead compound (2-(2-quinolin-3-ylpyridin-4-yl)-1,5,6,7-tetrahydro-4*H*-pyrrolo[3,2-*c*]pyridin-4-one), referred to as P4O herein.

Overall architecture of MK3

MK3 exhibits a typical bilobal protein kinase fold with an N-terminal lobe consisting of a core 5-stranded (β1-β5) β-sheet, a C-terminal lobe consisting mainly of α-helixes and a hinge region interconnecting the N- and C- terminal lobe (Fig. 1). MK3 appears to be in an active kinase conformation, with the catalytic residues Lys73, Glu84 and Asp187 in the same conformation to that seen in the active MK2/ADP structure (1NY3) to interact with ATP for phosphate transfer. Similar to MK2, MK3 also contains other features that are highly conserved including a 3 turn αC-helix (residues 79–92) and a glycine-rich loop (or P-loop, residues 51–56) with the conserved motif GXGXXG between the β1-β2 strand of the N-terminal lobe. The MK3 structure overall adopts a highly similar conformation to the MK2/P4O (2JBO) structure with rmsd between 221 Cα atoms of 0.56 Å (Fig. 2). However, some conformational flexibility of the glycine loops between MK3 and MK2 is observed. Similar to one of the MK2/P4O structures (2JBP chain A) in MK3 the glycine loop closes down towards the C-terminal lobe while in the other MK2 structures this movement was hindered by an intercalated sulphate ion present in the crystallization buffer (2JBO chain A), or by the presence of the β-phosphate of ADP (1NY3 chain A).[8] The glycine loop therefore has a more open conformation in these structures. The construct used in solving the MK3 structure contains a partially truncated C-terminal autoinhibitory domain including the NES. This domain is well defined in the structure, which contains a 2-turn (αJ) and a 4-turn (αK) α-helix and an extended C-terminal tail (residue 345–349) which is stabilized via crystal contact with the N-terminal lobe of a symmetry-related molecule. The αK helix extends across the surface of the C-terminal lobe and sterically blocks the substrate binding site, with the side chain nitrogen of Arg343 forming a hydrogen bond to the side chain (2.9 Å) and backbone carbonyls (2.7 Å) of Asp166 and Arg165, respectively. In the active MK2/ADP (1NY3) or MK2/staurosporine (1NXK) structures this C-terminal autoinhibitory domain is disordered[8] while in the inactive autoinhibited MK2 structure (1KWP) this region adopts a similar α-helical conformation which occupies the same position in space.[7] It is possible that in our MK3 structure the helical conformation of the C-terminal region is due

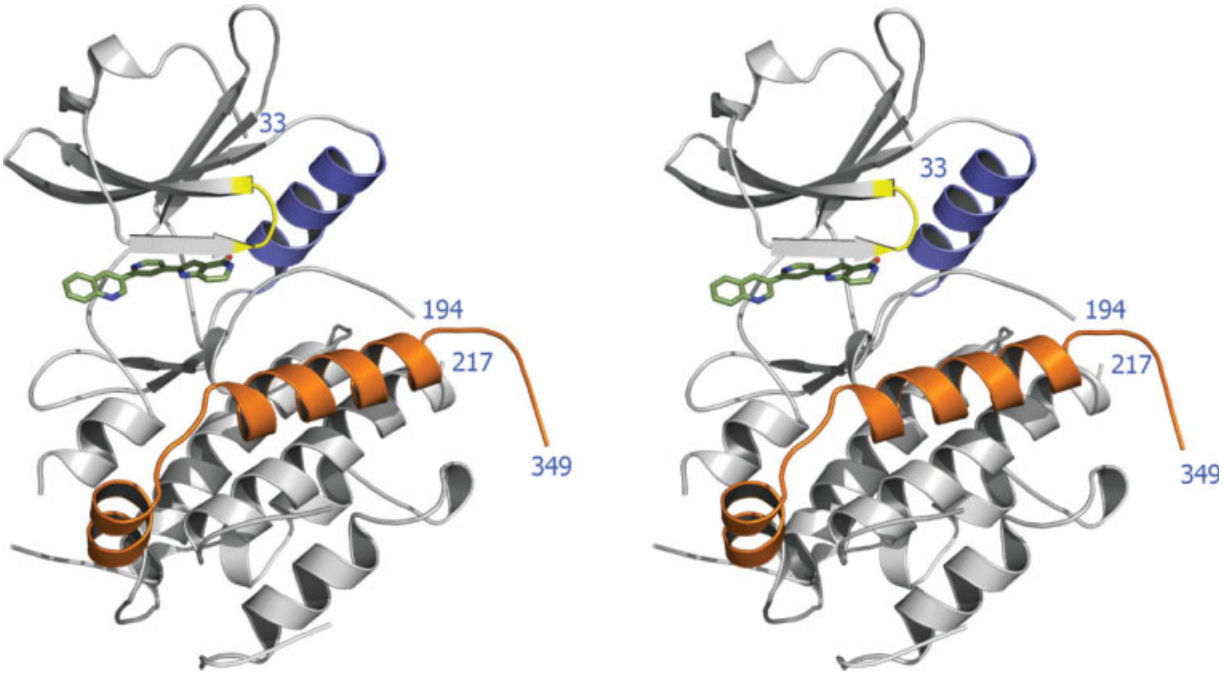

Figure 1. Stereo diagram of the overall architecture of MK3 with inhibitor bound. Secondary structures are represented as helix (α-helix), arrow (β-sheet), loops (disordered loop). Most of the activation loop is disordered and is not shown in the figure but the residues flanking this disordered region are labeled. The glycine-rich loop GLGVNG is colored in yellow; αC helix in purple; C-terminal auto-inhibitory domain in orange. The ligand P4O is in stick representation.

to the stabilization effect contributed by the crystal contact of the extreme C-terminus.

In protein kinases the activation loop governs kinase activation and substrate binding. Activation of MK2/3 requires phosphoryation of a threonine residue (Thr201 in MK3) in the activation loop. In the MK3 structure most of the activation loop (residues 195–216), including Thr201, is disordered indicating that this segment is highly mobile in the structure. Mass spectrometry data indicated that this MK3 construct is not phosphorylated. The side chain phenyl of Phe188 (the Phe of DFG) is oriented towards Ala91 of the αC-helix (so called DFG "in" conformation). In the MK2/ADP and MK2/staurosporine structure the activation loop is partially stabilized by crystal contact, however the putative phosphorylation site (Thr220) is disordered in the electron density map.[8] Another region disordered in the MK3 structure is between residues 243–263 in the C-terminal lobe, which contains disordered loops and a 2-turn α-helix (αG) in the MK2 structure.

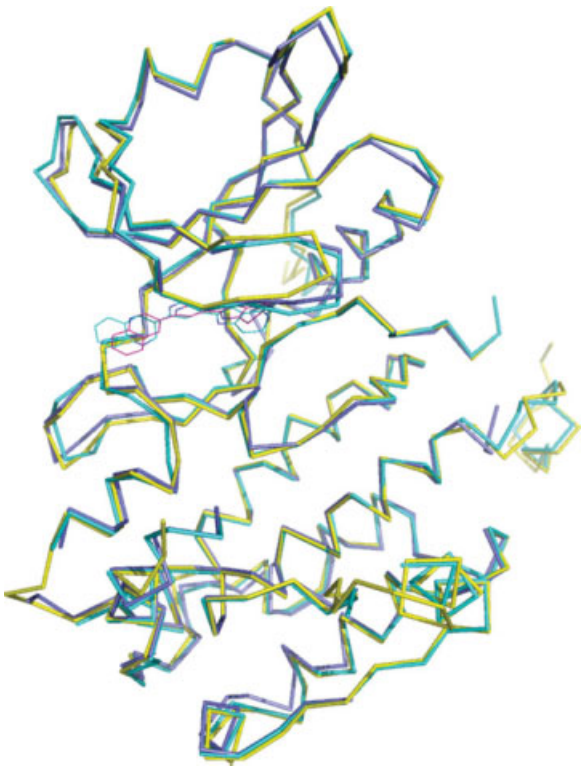

Figure 2. Superimposition of the MK2 (2JBO: yellow)/MK2 (2JBP: cyan)/MK3 (blue) backbone structure in ribbon representation with the same inhibitor bound (cyan in MK3 and pink in MK2). For clarity purpose residues 329–349 of MK3 which were not observed in both MK2 structures were omitted. Superimposition was performed and the figure generated in Pymol.[13]

Binding mode interaction of P4O with MK3

P4O sits in the ATP binding cleft between the N- and C-terminal lobes of MK3 (Fig. 1). P4O is a planar, boomerang-shaped molecule and mimics ATP binding with the pyridin-4-yl ring occupying the same position as the adenine moiety of ATP (Fig. 3). P4O is a classical ATP-competitive inhibitor[14] that forms a key hydrogen bond (2.9 Å) to the backbone

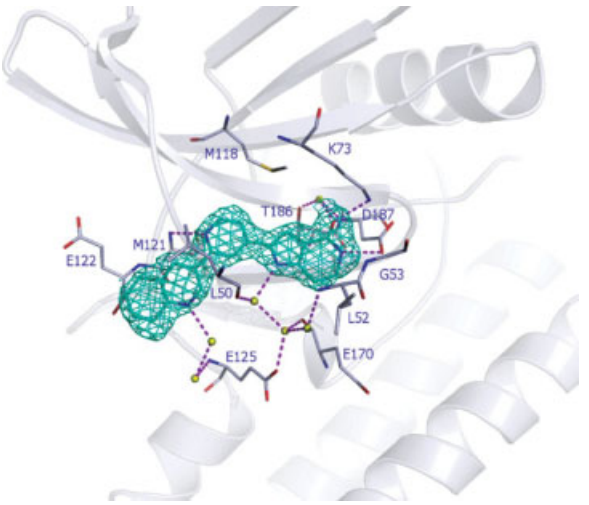

Figure 3. Schematic diagram of P4O interaction with residues in the active site pocket and water molecules at the opening of the ATP binding pocket of MK3. The ligand makes few direct interactions but contact MK3 residues via coordination by a network of water molecules. Hydrogen bond contacts as discussed in text are depicted as dotted line (purple). Water molecules are depicted as yellow spheres. MK3 active site residues are colored in white while P4O is in cyan. The initial fofc electron density map (before ligand is built) for P4O contoured at 2.0σ is colored in cyan. Figure generated in Pymol.

amide of Met 121 of the hinge region via the nitrogen of the pyridin-4-yl ring.

P4O forms a limited number of additional hydrogen bonds to the active site residues of MK3. The carbonyl oxygen on the pyrrolo pyridine ring contacts the terminal ε-amino group of Lys73 (2.9 Å) (Fig. 3). Binding of P4O forces Asp187 into an unfavorable conformation due to the presence of the bulky 1, 5,6,7-tetrahydro-4*H*-pyrrolo[3,2-*c*]pyridin-4-one ring. MK3 has Met118 (Met138 in MK2) as the gatekeeper residue at the back of the ATP binding pocket but P4O does not make contacts to this residue in either our MK3 or the MK2 structure.

P4O contacts MK3 active site residues via a network of coordinated water molecules, which become visible at the high resolution of the structure. The carbonyl oxygen of the 1,5,6,7-tetrahydro-4*H*-pyrrolo[3,2-*c*]pyridin-4-one ring contacts the backbone amide of Asp187 and side chain oxygen of Thr186 in the back of the ATP binding pocket via a bridging water molecule (Fig. 3). The pyrrole nitrogen indirectly contacts the backbone carbonyl oxygen of Leu50 on the β1 strand via another bridging water molecule. This water molecule belongs to a network of coordinated water molecules at the opening of the ATP binding pocket that elicits hydrogen bond interaction of P4O with the backbone atoms of Leu50 and Leu52 in the β1 strand (driving the closing of the glycine-rich loop) and Glu125 and Glu170 in the C-terminal lobe. As a result of the closing of the glycine-rich loop Gly53 now occupies the position of the β-phosphate of ADP as seen in the MK2/ADP structure. Binding of P4O therefore induces the formation of a deep and narrow ATP binding pocket in MK3.

The nitrogen of the quinolin-3-yl heterocycle is oriented towards the solvent. It forms a hydrogen bond with a water molecule that belongs to the network of water molecules at the opening of the ATP binding pocket (Fig. 3). The electron density observed for this water is weaker than the other water molecules in the same interaction network (visible at 1δ but disappeared at 1.5δ of a 2fo-fc map). However, the water seems to play a role in dictating the orientation of the quinolin-3-yl ring system. In the MK2/P4O structures (2JBO, 2JBP) water molecules were not clearly defined at the resolution of the structures and the quinolin-3-yl heterocycle is in the opposite orientation to that seen in our MK3 structure. This discrepancy could be due to the difference in the resolution of the structures or genuine difference in the binding mode of P4O in the active site of MK2 and MK3. The latter explanation is supported by the difference in experimental IC_{50} values of P4O for MK2 and MK3 of 8.5 and 210 n*M*, respectively.

Difference between MK2/MK3 binding pocket

MK2 and MK3 are highly homologous kinases and the amino acid residues around the two active sites are particularly well conserved. The MK3/P4O and MK2/P4O (2BJP chain A) structures superimpose very well with rmsd between 273 Cα atoms of 0.68 Å. P4O occupies the same position in the active site in both MK2 and MK3 making very similar contacts but with the quinolin-3-yl ring system flipped by 180°. There is a slight difference between the ATP binding pockets of MK2/MK3 as characterised by a couple of conservative changes at the hinge region. Met121 (MK3) whose side chain protrudes at the bottom of the adenine pocket is replaced with Leu141 (MK2). Glu122 (MK3) whose side chain points towards the solvent is replaced with a similarly negatively charged but less bulky Asp142 residue (MK2). Neither residue is directly involved with ligand or nucleotide binding as is observed in both other structures and our MK3 structure and hence it would seem unlikely these conservative changes will confer any significant difference in ligand interaction between MK2/MK3.

Discussion

MK2 and MK3 are closely related kinases in sequence, secondary and tertiary structure, as well as function. It is unclear at present how exactly these two kinases play distinct roles in the physiological and pathophysiological setting. Based on the corresponding knock-out studies in mice we consider MK2 to be the dominant pro-inflammatory regulator with MK3 having a compensatory function that only

surfaces under conditions of MK2 absence. In this article we report the first crystal structure of MK3, which is also the first high resolution structure of the MK2/MK3 protein kinase family. Our structure confirms that MK3 has an active site pocket that closely resembles that of MK2, with conservative residue changes that are not directly involved in ligand interaction. Examination of the structure also reveals intricate detail around the active site pocket such as the water interaction network that has not been previously studied but could be instrumental in guiding structure-based drug design. From the perspective of drug discovery it would be extremely difficult to develop MK2 selective inhibitors (selective over MK3) but dual MK2 and MK3 inhibition may in fact be beneficial for pharmacological efficacy, given the redundant function. The structure of MK3 as described herein therefore opens an attractive avenue to the structure-based design of MK2/MK3 inhibitors. We and others have spent a considerable amount of effort to try to improve the crystallographic resolution of MK2 beyond the published 2.6 to 3.2 Å limit but unfortunately we consistently failed. While the MK3 structure should serve as a useful surrogate in the design of selective inhibitors against MK2 and/or MK3, our current project work is aimed at generating a MK3 chimeric protein having all the MK2 active site residues within 4 to 6 Å distance from the pyrrolopyridinone-based ligand, which includes Met121MK3 to Leu141MK2, Glu122MK3 to Asp142MK2 immediately around the active site pocket, and Val54MK3 to Ile74MK2 at the glycine loop.

Material and Methods

Bacterial strains, enzymes and chemicals

E. coli strains NEB5α and Rosetta 2 (DE3) were obtained from New England Biolabs (Hitchin, UK) and Merck Biosciences (Nottingham, UK) respectively. Bacteria were grown at 37°C in 2xYT media (Anachem, Luton, UK) unless otherwise stated. Plasmid DNA was prepared using a CompactPrep DNA purification kit (Qiagen, Crawley, UK). PCRs were set up using a Janus Workstation (Perkin–Elmer, Waltham) and run in a Piko 24-well thermocycler (Labtech International, Ringmer, UK) using Phusion polymerase (New England Biolabs, Hitchin, UK). InFusion cloning was carried out using an In-Fusion CF Dry-Down PCR Cloning Kit (Clontech-Takara Bio Europe, Saint-Germain-en-Laye, France). DNA sequencing was performed using a BigDye Terminator v1.1 cycle sequencing kit (Applied Biosystems, Warrington, UK) and analyzed at Cogenics Inc. (Takeley, UK). Gene synthesis was carried out by Geneart AG (Regensburg, Germany), with the codon-usage optimized for *E. coli* expression. Compound P4O (2-(2-quinolin-3-ylpyridin-4-yl)-1,5,6,7-tetrahydro-4*H*-pyrrolo[3,2-*c*]pyridin-4-one) was prepared following literature methods [compound 16 in (13)].

Construction of MK3 expression plasmids

See (Supporting Information Table 1) shows the PCR primers used in the construction of expression constructs EV236-EV259 encoding MK3 with varying N- and C- termini. The constructs EV236-EV253 (Supporting Information Table 2) were amplified by PCR, using a synthetic gene of full-length MK3 as the template DNA, and cloned into the vector pTriIJ-POPIN (digested with *KpnI* and *HindIII*) using InFusion cloning. Similarly, EV254 and EV255 were PCR amplified and cloned into pTriIJ-POPIN digested with *NcoI* and *PmeI*. Finally, a synthetic gene was made encoding residues Gln-41 to Ile-54 of MK2 linked in frame to residues Lys-35 to Gln-382 of MK3. This was used as template DNA for PCR of the chimera EV256-EV259. The PCR products were cloned using InFusion into the vector pTriIJ-POPIN digested with *KpnI* and *HindIII*. The InFusion reaction mixtures were used to transform *E. coli* NEB5α and transformants were selected using carbenicillin (100 μg/mL). After verifying the DNA sequences, plasmid DNA containing the correct insert was transformed into *E. coli* strain Rosetta 2 (DE3).

Expression and purification of MK3 constructs

Rosetta 2 (DE3) cells containing the MK3 plasmids were grown in 2xYT media (2L culture) supplemented with 100 μg/mL carbenicillin to an optical density at 600 nm of 0.6. IPTG was added to a final concentration of 0.5 m*M* and the cells were incubated for a further 16 hours at 20°C, after which they were harvested by centrifugation at 5000*g* for 15 minutes.

Each *E. coli* Rosetta 2 (DE3) cell pellet (9.5 g wet weight), harboring the MK3 construct of choice, was resuspended in 50 mL ice-cold buffer A (50 m*M* Tris pH8.8, 300 m*M* NaCl and 1 m*M* DTT) supplemented with 'Complete' tablet-EDTA free (Roche) and 3 μL benzonase (Merck, 250 U/μL). The cells suspension was lysed using a cell disruptor (25 Psi) and clarified by centrifugation (25,000*g*, 45 min at 4°C). The cleared lysate was loaded on a His-Trap affinity chromatography column pre-equilibrated with buffer A. The column was washed with buffer A containing 10 m*M* imidazole and the protein eluted using 300 m*M* imidazole. The collected fraction was bound to a Hi-Trap Q anion exchange column pre-equilibrated with buffer B (50 m*M* Tris pH 8.0, 1 m*M* DTT) and the protein eluted over a gradient of 0 to 1 *M* NaCl in buffer B. The fractions containing MK3 were analyzed by SDS-PAGE and visualized by Coomassie Blue staining. The purest and most concentrated fractions were pooled and cleaved with HRV 3C protease (Novogen) using 5 U/mg of protein (buffer B, overnight at 4°C with gentle

rocking). The His-tagged protease and any uncleaved MK3 fusion protein were removed by a second Ni^{2+}-NTA affinity chromatography step. The untagged protein was collected and loaded on a size exclusion chromatography column (Superdex 75, 16/60) equilibrated in 20 m*M* Tris pH7.5, 200 m*M* NaCl, 1 m*M* DTT. The eluted fractions were analyzed by SDS-PAGE and the purest fractions were pooled, concentrated and diafiltered into buffer B. The protein was further purified by high resolution ion exchange chromatography on a Mono-Q column pre-equilibrated in buffer B. After SDS-PAGE analysis the fractions containing pure MK3 were pooled and the buffer exchanged into a final storage buffer (20 m*M* Tris pH7.5, 200 m*M* NaCl, 10 m*M* DTT). The protein was concentrated to 7.5 mg/mL and stored at −70°C for further use.

Crystallization of MK3 and soaking

Crystals of MK3 were grown at room temperature using the sitting drop vapor diffusion method. MK3 construct EV242 (amino acids 33–349) at 7.5 mg/mL was mixed with 0.5 m*M* P4O [compound 16 in (13)] and 10 m*M* DTT and incubated on ice for 1hr. 250 nL of the mixture was then mixed with 50 nL of mother liquor containing 100 m*M* Bis-Tris propane/citric acid pH 5.0, 10–21% PEG3350 over 60 μL reservoir solution. Crystal forms in spacegroup C2 with unit cell dimension $a = 84.7$Å $b = 74.8$ Å $c = 60.7$ Å $\alpha = 90.0°$ $\beta = 107.3°$ $\gamma = 90.0°$. Plate-like crystals grow to a maximum dimension of 100 μm × 100 μm over few days.

Data collection and processing

The dataset was collected at the Diamond beamline I02 using an ADSC Q315 CCD detector. For the MK3/P4O complex, the crystal was cryoprotected in mother liquor supplemented with 20% 2-methyl-2,4-pentanediol (MPD) and frozen to 100K. The crystal diffracted and was processed to a resolution of 1.9 Å. Diffraction data were integrated and scaled using the CrystalClear processing suite (Rigaku). The structure was solved using an in-house MK2 structure (residues 46–350) as a molecular replacement search model using Phaser.[15] There is one molecule per asymmetric unit giving a solvent content of 51.8%. The initial model was rebuilt using COOT[16] and refined using REFMAC.[17] After three refinement cycles the ligand P4O was built into the refined model. The model was further refined in REFMAC giving an R factor of 0.23 (R_{free} 0.27). The final model contains amino acid residues 33–349 of MK3 (with residues 134, 195–216, 243–263 missing), one molecule of P4O and 161 water molecules. The final statistics for data collection and processing are listed in (Supporting Information Table 3). The coordinates have been deposited into the Protein Data Bank under accession code 3FHR.

References

1. Gaestel M, Mengel A, Bothe U, Asadullah K (2007) Protein kinases as small molecule inhibitor targets in inflammation. Curr Med Chem 14:2214–2234.
2. Duraisamy S, Bajpai M, Bughani U, Dastidar SG, Ray A, Chopra P (2008) MK2: a novel molecular target for anti-inflammatory therapy. Expert Opin Ther Targets 12:921–936.
3. Ronkina N, Kotlyarov A, Gaestel M (2008) MK2 and MK3–a pair of isoenzymes? Frontiers Biosci 13:5511–5521.
4. Hegen M, Gaestel M, Nickerson-Nutter CL, Lin LL, Telliez JB (2006) MAPKAP kinase 2-deficient mice are resistant to collagen-induced arthritis. J Immunol 177:1913–1917.
5. Kotlyarov A, Neininger A, Schubert C, Eckert R, Birchmeier C, Volk HD, Gaestel M (1999) MAPKAP kinase 2 is essential for LPS-induced TNF-alpha biosynthesis. Nat Cell Biol 1:94–97.
6. Ronkina N, Kotlyarov A, Dittrich-Breiholz O, Kracht M, Hitti E, Milarski K, Askew R, Marusic S, Lin LL, Gaestel M, Telliez JB (2007) The mitogen-activated protein kinase (MAPK)-activated protein kinases MK2 and MK3 cooperate in stimulation of tumor necrosis factor biosynthesis and stabilization of p38 MAPK. Mol Cell Biol 27:170–181.
7. Meng W, Swenson LL, Fitzgibbon MJ, Hayakawa K, Ter Haar E, Behrens AE, Fulghum JR, Lippke JA (2002) Structure of mitogen-activated protein kinase-activated protein (MAPKAP) kinase 2 suggests a bifunctional switch that couples kinase activation with nuclear export. J Biol Chem 277:37401–37405.
8. Underwood KW, Parris KD, Federico E, Mosyak L, Czerwinski RM, Shane T, Taylor M, Svenson K, Liu Y, Hsiao CL, Wolfrom S, Maguire M, Malakian K, Telliez JB, Lin LL, Kriz RW, Seehra J, Somers WS, Stahl ML (2003) Catalytically active MAP KAP kinase 2 structures in complex with staurosporine and ADP reveal differences with the autoinhibited enzyme. Structure 11:627–636.
9. Malawski GA, Hillig RC, Monteclaro F, Eberspaecher U, Schmitz AAP, Crusius K, Huber M, Egner U, Donner P, Mueller-Tiemann B (2006) Identifying protein construct variants with increased crystallization propensity–a case study. Protein Sci 15:2718–2728.
10. Hillig RC, Eberspaecher U, Monteclaro F, Huber M, Nguyen D, Mengel A, Muller-Thiemann B, Egner U (2007) Structural basis for a high affinity inhibitor bound to protein kinase MK2. J Mol Biol 369:735–745.
11. Argiriadi MA, Sousa S, Banach D, Marcotte D, Xiang T, Tomlinson MJ, Demers M, Harris C, Kwak S, Hardman J, Pietras M, Quinn L, Dimauro J, Ni B, Mankovich J, Borhani DW, Talanian RV, Sadhukhan R (2009) Rational mutagenesis to support structure-based drug design: MAPKAP kinase 2 as a case study. BMC Struct Biol 9:16.
12. Ter Haar E, Prabakhar P, Liu X, Lepre C (2007) Crystal structure of the p38 alpha-MAPKAP kinase 2 heterodimer. J Biol Chem 282:9733–9739.
13. DeLano WL (2002) http://www.pymol.org.
14. Anderson DR, Meyers MJ, Vernier WF, Mahoney MW, Kurumbail RG, Caspers N, Poda GI, Schindler JF, Reitz DB, Mourey RJ (2007) Pyrrolopyridine inhibitors of mitogen-activated protein kinase-activated protein kinase 2 (MK-2). J Med Chem 50:2647–2654.
15. Mccoy AJ, Grosse-Kunstleve RW, Adams PD, Winn MD, Storoni LC, Read RJ (2007) Phaser crystallographic software. J Appl Cryst 40:658–674.
16. Emsley P, Cowtan K (2004) Coot: model-building tools for molecular graphics. Acta Cryst 60:2126–2132.
17. Murshudov GN, Vagin AA, Dodson EJ (1997) Refinement of macromolecular structures by the maximum-likelihood method. Acta Cryst 53:240–255.